

Supporting Information

© Wiley-VCH 2011

69451 Weinheim, Germany

**Titania Supported Iridium Subnanoclusters as an Efficient Heterogeneous Catalyst for Direct Synthesis of Quinolines from Nitroarenes and Aliphatic Alcohols\*\***

*Lin He, Jian-Qiang Wang, Ya Gong, Yong-Mei Liu, Yong Cao,\* He-Yong He, and Kang-Nian Fan*

anie\_201104089\_sm\_miscellaneous\_information.pdf

## Supporting Information

### 1. Catalytic materials

**Preparation of catalysts:** 1 wt % Ir/TiO<sub>2</sub>-NPs, 1 wt % Ir/CeO<sub>2</sub>, 1 wt % Ir/ZnO, 1 wt % Ir/SiO<sub>2</sub>, 1 wt % Pt/TiO<sub>2</sub>, 1 wt % Pd/TiO<sub>2</sub>, 1 wt % Ru/TiO<sub>2</sub>, 1 wt % Ag/TiO<sub>2</sub> samples were prepared by a classical incipient wetness impregnation (IWI) method. H<sub>2</sub>IrCl<sub>6</sub>·6H<sub>2</sub>O (Aldrich), H<sub>2</sub>PtCl<sub>6</sub>·6H<sub>2</sub>O (Aldrich), PdCl<sub>2</sub> (Aldrich), RuCl<sub>3</sub> (Aldrich) and AgNO<sub>3</sub> (Aldrich) precursors were used to impregnate the TiO<sub>2</sub> (Evonik P25), CeO<sub>2</sub> (Evonik Adnano 90), ZnO (Merck Chemicals) and SiO<sub>2</sub> (Evonik Aerosil 380) supports. As an example, 2 g of TiO<sub>2</sub> was added to 2 mL of an aqueous solution containing appropriate amounts of H<sub>2</sub>IrCl<sub>6</sub>·6H<sub>2</sub>O to prepare the 1 wt % Ir/TiO<sub>2</sub>-NPs. After a perfect mixing of the corresponding slurries, samples were dried at 80 °C for 5 h and then reduced in 5 vol % H<sub>2</sub>/Ar at 400 °C for 2 h. In the case of the 1 wt % Au/TiO<sub>2</sub> catalyst, a routine deposition-precipitation (DP) procedure<sup>[S1]</sup> has been employed to deposit gold nanoparticles onto the TiO<sub>2</sub> support. The mean size of different metal nanoparticles on various supports (1 wt %) was in the range of 1.5-2.5 nm (see TEM data in Fig. S1). 5 wt % Ir/TiO<sub>2</sub>, 0.05 wt % Ir/TiO<sub>2</sub>-NCs samples were prepared by incipient wetness technique at the desired metal contents. As for 0.05 wt % Ir/TiO<sub>2</sub>-NCs, most of the Ir species was in the region of subnanometers (ca. 0.9 nm, denoted as Ir/TiO<sub>2</sub>-NCs, see Figure S2 and Table S3).

### 2. Catalytic activity measurements

**2.1 General procedure for the direct synthesis of quinolines from nitroarenes and aliphatic alcohols:** A mixture of nitrobenzene (5 mmol), alcohol (20 mL), and catalyst (metal: 0.167 mol %) was charged into an autoclave (100 mL capacity). The resulting mixture was vigorously stirred (1000 rpm with a magnetic stir bar) at 120 °C under N<sub>2</sub> atmosphere (5 atm) for given reaction time. The products were confirmed by the comparison of their GC retention time, mass, and <sup>1</sup>H and <sup>13</sup>C NMR spectroscopy. The conversion and product selectivity were determined by a GC-17A gas chromatograph equipped with a HP-5 column (30 m × 0.25 mm) and a flame ionization detector (FID). For isolation, the combined organic layer was dried over anhydrous Na<sub>2</sub>SO<sub>4</sub>, concentrated, and purified by silica gel column chromatography.

**2.2 Recovery and reuse of Ir/TiO<sub>2</sub>-NCs:** The reused catalyst was recovered by centrifuging the solid Ir/TiO<sub>2</sub>-NCs from liquid phase after reaction. The recovered catalyst was washed with propanol for several times. The catalyst was then dried under vacuum at room temperature for 12 h. In the three successive cycles, the yields of 2-ethyl-3-methylquinoline (**3a**) were 86%, 76%, and 71% (GC analysis), respectively.

**2.3 Direct conversion of aniline and aldehyde over Ir/TiO<sub>2</sub>-NCs:** A mixture of aniline (5 mmol), propanal (20 mmol), tert-butanol (20 mL), and Ir/TiO<sub>2</sub>-NCs (Ir: 0.167 mol %) was charged into an autoclave (100 mL capacity). The resulting mixture was vigorously stirred (1000 rpm with a magnetic stir bar) at 120 °C under N<sub>2</sub> atmosphere (5 atm) for 8 h. The yield of 2-ethyl-3-methylquinoline (**3a**) was 67% (GC analysis).

**2.4 Direct conversion of aniline and 2-methyl-2-pentenal over Ir/TiO<sub>2</sub>-NCs:** A mixture of aniline (5 mmol), 2-methyl-2-pentenal (10 mmol), tert-butanol (20 mL), and Ir/TiO<sub>2</sub>-NCs (Ir: 0.167 mol %) was charged into an autoclave (100 mL capacity). The resulting mixture was vigorously stirred (1000 rpm with a magnetic

stir bar) at 120 °C under N<sub>2</sub> atmosphere (5 atm) for 8 h. The yield of 2-ethyl-3-methylquinoline (**3a**) was 59% (GC analysis).

**2.5 Direct conversion of aniline and aldehyde over different Ir-free supports:** A mixture of aniline (5 mmol), propanal (20 mmol), tert-butanol (20 mL) and support (refer to TiO<sub>2</sub>, CeO<sub>2</sub>, ZnO or SiO<sub>2</sub>, 160 mg) was charged into an autoclave (100 mL capacity). The resulting mixture was vigorously stirred (1000 rpm with a magnetic stir bar) at 120 °C under N<sub>2</sub> atmosphere (5 atm) for given reaction time. The results were depicted in Table S1.

**2.6 The examination of a series of Ir/TiO<sub>2</sub> samples for the direct synthesis of quinolines:** A mixture of nitrobenzene (5 mmol), alcohol (20 mL), and catalyst (refer to 0.05 wt % Ir/TiO<sub>2</sub>-NCs, 1 wt % Ir/TiO<sub>2</sub>-NPs, and 5 wt % Ir/TiO<sub>2</sub> samples, Ir: 0.167 mol %) was charged into an autoclave (100 mL capacity). The resulting mixture was vigorously stirred (1000 rpm with a magnetic stir bar) at 120 °C under N<sub>2</sub> atmosphere (5 atm) for 1 h.

**2.7 50-mmol scale tandem synthesis of quinoline:** A mixture of nitrobenzene (50 mmol), propanol (50 mL), and Ir/TiO<sub>2</sub>-NCs (Ir: 0.0167 mol %) was charged into an autoclave (200 mL capacity). The resulting mixture was vigorously stirred (1000 rpm with a magnetic stir bar) at 120 °C under N<sub>2</sub> atmosphere (5 atm) for given reaction time.

**2.8 The synthesis of 2-alkenyl bis-quinoline from 2-methylquinoline and quinaldehyde:** A mixture of 2-methylquinoline (5 mmol), quinaldehyde (5 mmol, prepared from the corresponding methylquinoline by oxidation with selenium dioxide in refluxing xylene<sup>[S2]</sup>), acetic anhydride (4 mL) and acetic acid (2 mL) was charged into a round bottom flask (25 mL capacity), equipped with a condenser, under a N<sub>2</sub> atmosphere (1 atm). The reaction mixture was vigorously stirred (1000 rpm with a magnetic stir bar) at 110 °C for 16 h. After reaction, the product was poured into excess aqueous sodium hydroxide and the mixture extracted with toluene (3\*50 mL). The combined organic layers were washed with brine and dried over MgSO<sub>4</sub>. After filtration and concentration, the crude product was purified by crystallization in ethanol to afford the desired product.

**Table S1** Direct conversion of aniline and aldehyde to 2-ethyl-3-methyl-1,2-dihydroquinoline (**2a**) intermediate over different Ir-free supports

Entry	Catalyst	Conversion (%)	Yield (%)
1	TiO <sub>2</sub>	59	41
2	CeO <sub>2</sub>	27	16
3	ZnO	19	12
4	SiO <sub>2</sub>	7	4

Reaction conditions: aniline (5 mmol), propanal (20 mmol), tert-butanol (20 mL), support (refer to TiO<sub>2</sub>, CeO<sub>2</sub>, ZnO or SiO<sub>2</sub>, 160 mg), at 120 °C under N<sub>2</sub> atmosphere (5 atm) for 8 h. In all cases, the main by-product was Schiff base formed from aniline and aldehyde. Notably, only trace of desired 2-ethyl-3-methylquinoline (**3a**) was detected under present Ir-free conditions.

**Table S2** The examination of a series of Ir/TiO<sub>2</sub> samples for the direct synthesis of 2-ethyl-3-methylquinoline (**3a**)<sup>[a]</sup>

Entry	catalyst	Ir particle size (nm) <sup>[b]</sup>	Ir dispersion <sup>[c]</sup>	Conversion (%) <sup>[d]</sup>	Yield (%) <sup>[d]</sup>	TOF (h <sup>-1</sup> ) <sup>[d]</sup>
1	Ir/TiO <sub>2</sub> -NCs (0.05 wt %)	0.9	0.96	29	23	181
2	Ir/TiO <sub>2</sub> -NPs (1 wt %)	1.5	0.78	22	16	169
3	Ir/TiO <sub>2</sub> (5 wt %)	2.3	0.51	11	3	129

[a] Reaction conditions: Nitrobenzene (5 mmol), propanol (20 mL), catalyst (Ir: 0.167 mol %) at 120 °C under N<sub>2</sub> atmosphere (5 atm) for 1 h. [b] Ir particle size was determined by transmission electron microscope (TEM) micrographs or high resolution transmission electron microscopy (HRTEM) ( see Figure S1 and Figure S2 ). [c] Ir dispersions were determined by H<sub>2</sub> chemisorption experiments ( see experimental details in characterization of catalysts section). [d] Conversions and yields were based on nitrobenzene consumption (GC analysis). The turn over frequency (TOF) was calculated on the basis of surface Ir atom determined by the Ir dispersion.

### 3. Characterization of catalysts

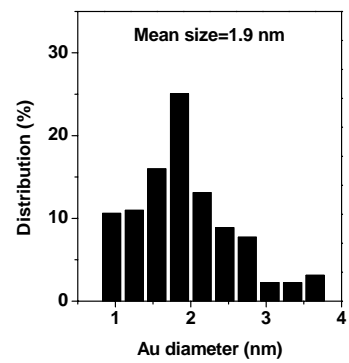
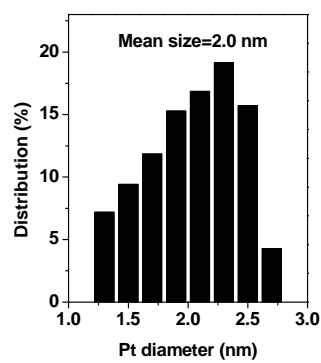
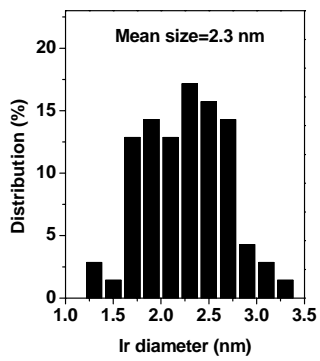
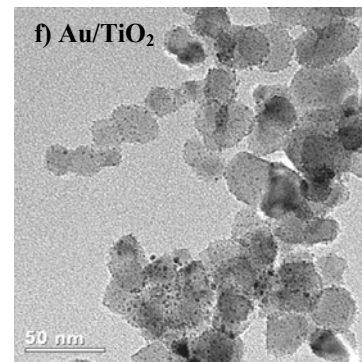
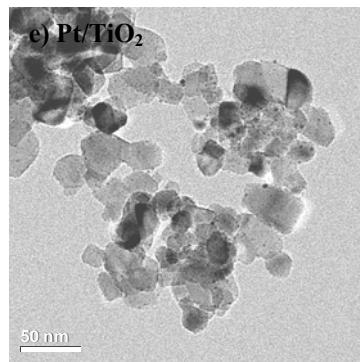
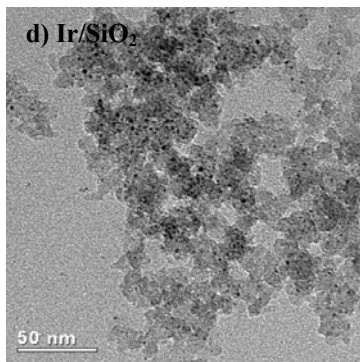
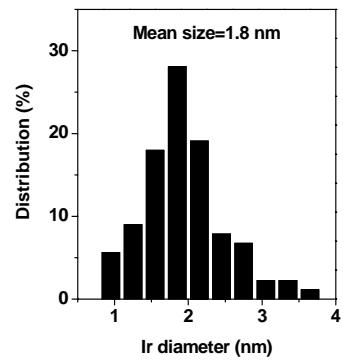
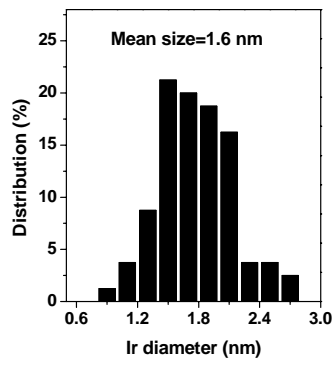
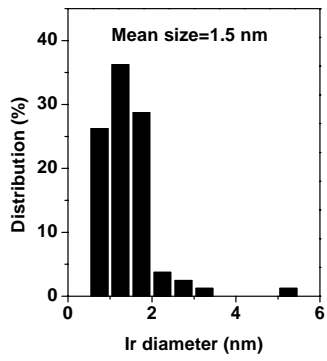
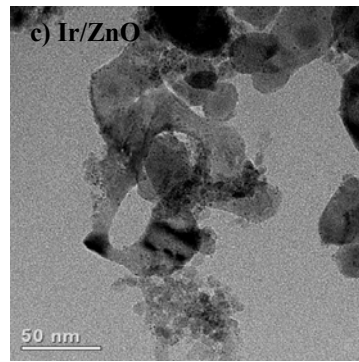
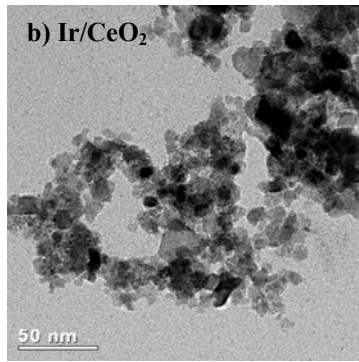
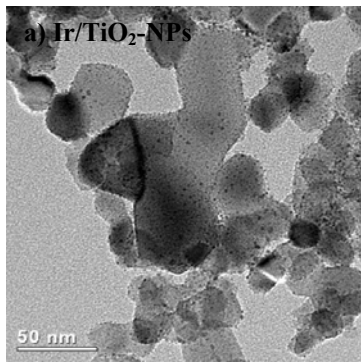
**3.1 Elemental analysis:** The metal loading of the catalysts was measured by inductively coupled plasma atomic emission spectroscopy (ICP-AES) using a Thermo Electron IRIS Intrepid II XSP spectrometer.

**3.2 Transmission electron microscopy (TEM):** TEM images for catalysts were taken with a JEOL 2011 electron microscope operating at 200 kV. Before being transferred into the TEM chamber, the samples dispersed with ethanol were deposited onto a carbon-coated copper grid and then quickly moved into the vacuum evaporator. The size distribution of the metal nanoclusters was determined by measuring about 200 random particles on the images.

**3.3 High resolution transmission electron microscopy (HRTEM):** HRTEM images for catalysts were taken with a JEM-2100F electron microscope operating at 200 kV. The size distribution of the metal nanoclusters was determined by measuring about 200 random particles on the images.

**3.4 Extended X-ray absorption fine structure (EXAFS):** The X-ray absorption data at the Ir  $L_3$ -edge of the samples were recorded at room temperature in transmission mode using ion chambers or in the fluorescent mode with silicon drift fluorescence detector at beam line BL14W1 of the Shanghai Synchrotron Radiation Facility (SSRF), China. The station was operated with a Si (311) double crystal monochromator. During the measurement, the synchrotron was operated at energy of 3.5 GeV and a current between 150-210 mA. The photon energy was calibrated with standard Pt metal foil. Data processing was performed using the program ATHENA.<sup>[S3]</sup> All fits to the EXAFS data were performed using the program ARTEMIS.

**3.5 H<sub>2</sub> chemisorption experiments:** H<sub>2</sub> chemisorption experiments were carried out in an Auto Chem II chemisorption Analyzer. 0.5 g catalyst sample was firstly treated in a flow of 10 vol % H<sub>2</sub>/Ar at 400 °C for 1 h at a ramping rate of 5 °C /min. After purging with Ar for 10 min, the sample was cooled down to 50 °C in Ar before the chemisorption experiments were carried out. The adsorption of hydrogen was carried out by pulsing 10 vol % H<sub>2</sub>/Ar until saturation. Hydrogen consumption was detected by a thermal conductivity detector (TCD). Metallic dispersions were calculated by the ratio of the irreversible uptake to the total metal content assuming an H:Ir = 1:1 surface stoichiometry.



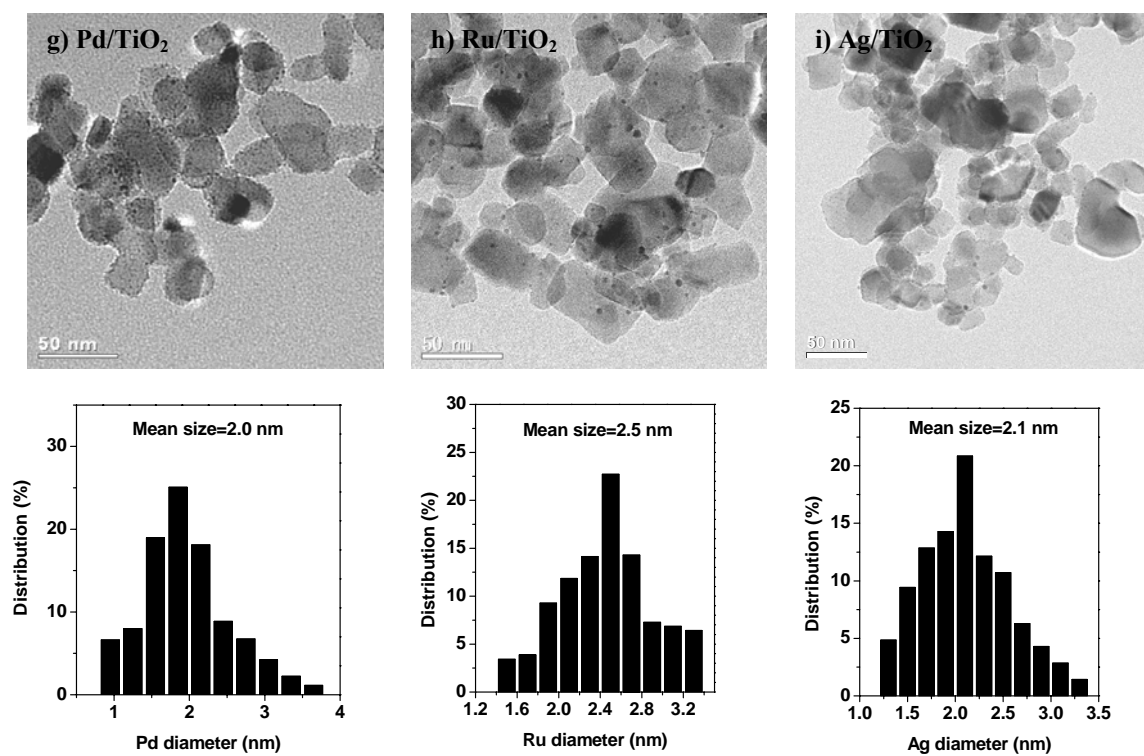


**Figure S1** Representative TEM image and size distribution of various catalysts

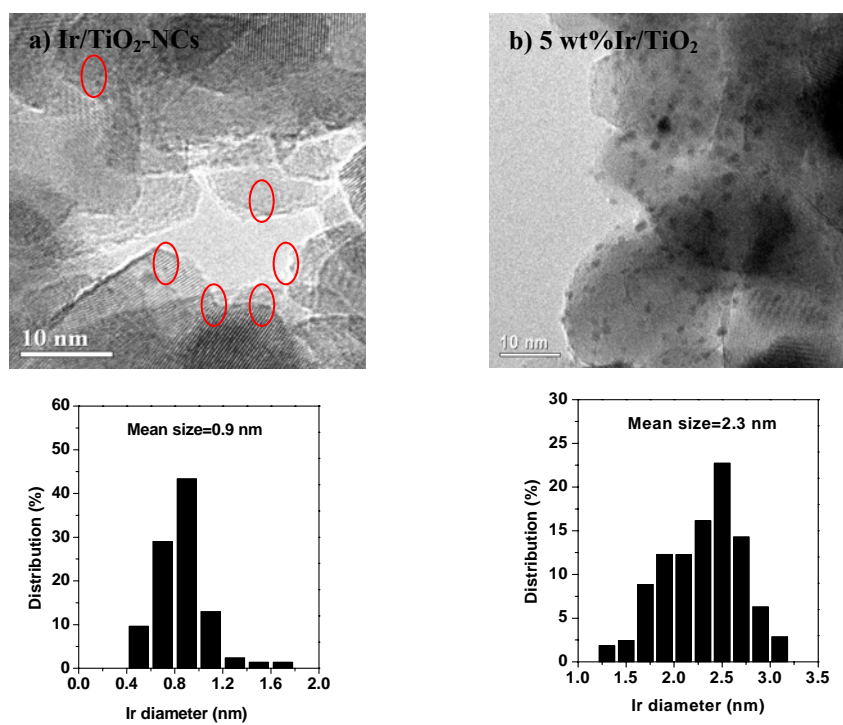


**Figure S2** Representative HRTEM image and size distribution of Ir/TiO<sub>2</sub>-NCs and 5 wt % Ir/TiO<sub>2</sub>

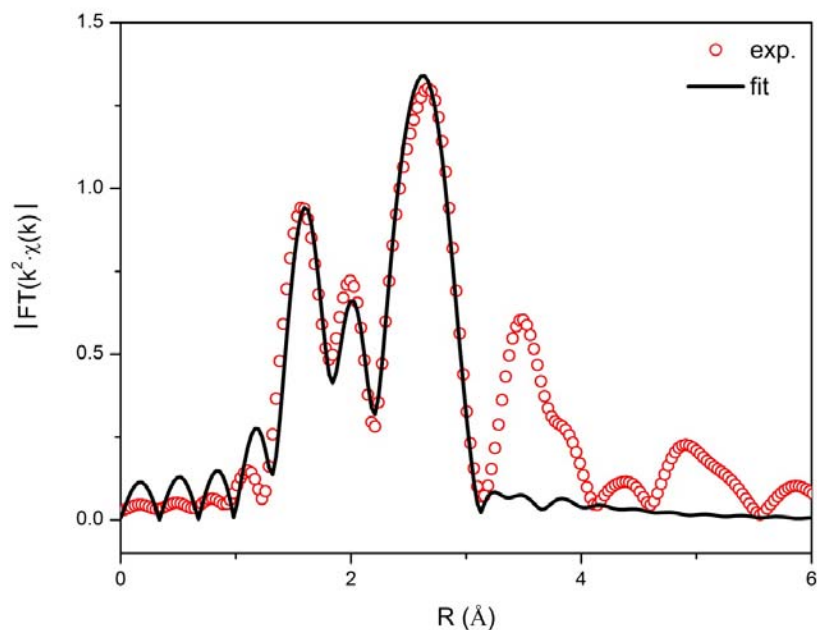


**Figure S3** Results of EXAFS data analysis characterizing of Ir/TiO<sub>2</sub>-NCs

**Table S3** Structural parameters characterizing Ir/TiO<sub>2</sub>-NCs as determined in the first-shell EXAFS analyses

Sample	Shell	N	R (Å)	$\sigma^2$ ( $10^{-3} \text{ \AA}^2$ )	$\Delta E_0$ (eV)
Ir/TiO <sub>2</sub> -NCs	Ir-O	1.3	1.98	2.0	7.4
	Ir-Ir	5.3	2.73	4.1	-10.3

Notation: **N**, coordination number; **R**, distance between absorber and backscatterer atoms;  $\sigma^2$ , Debye–Waller factor;  $\Delta E_0$ , inner potential correction. Error bounds (accuracies) characterizing the structural parameters obtained by EXAFS spectroscopy are estimated to be as follows: coordination number **N**,  $\pm 20\%$ ; distance **R**,  $\pm 0.02 \text{ \AA}$ ; Debye–Waller factor  $\sigma^2$ ,  $\pm 10\%$ ; and inner potential correction  $\Delta E_0$ ,  $\pm 20$ .

In Figure S3 and Table S3, the Fourier transform (FT) of the Ir  $L_3$  - edge EXAFS for the Ir/TiO<sub>2</sub>-NCs shows a peak at around 2.73 Å. This feature is due to the formation of Ir clusters with an average coordination number (*N*) of 5.3, corresponding to an Ir cluster size of  $\sim 0.9 \text{ nm}$  in diameter,<sup>[S4]</sup> which consists of with the result of the HRTEM (**Figure S2**) observation.

#### 4. The reaction profiles for the Ir/TiO<sub>2</sub>-NCs-catalyzed quinoline formation

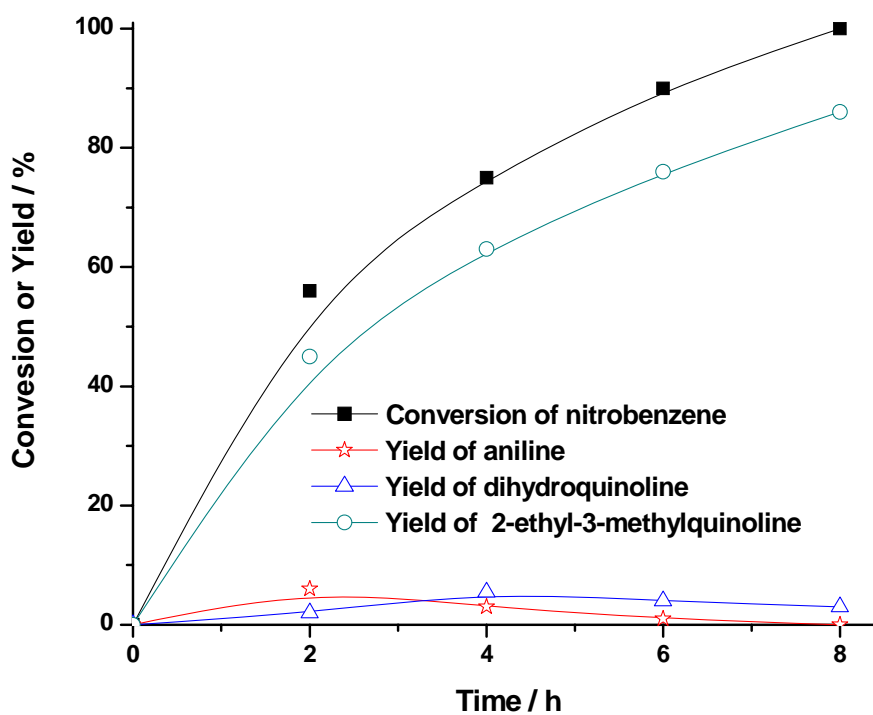
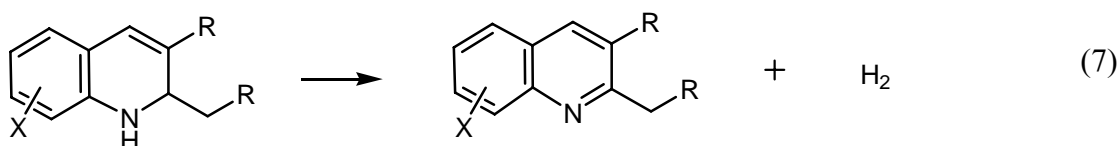
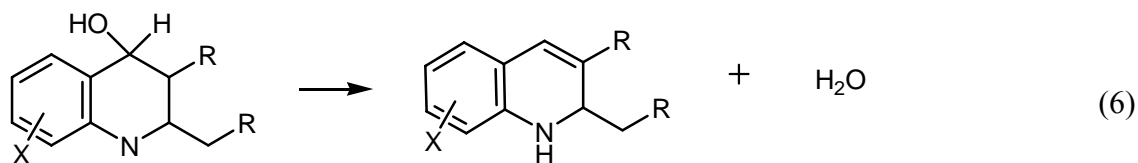
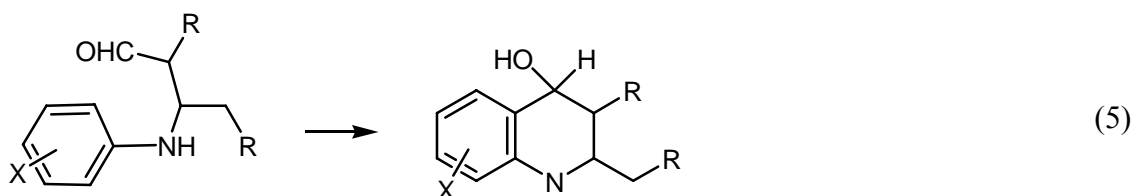
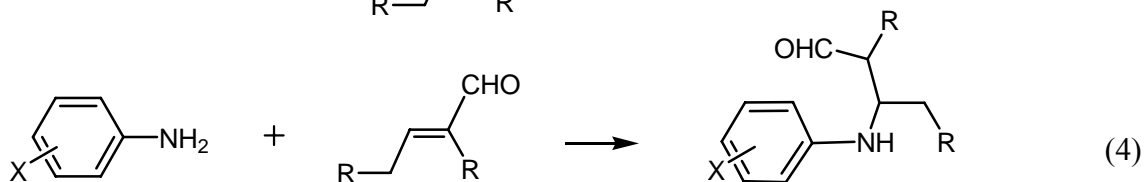
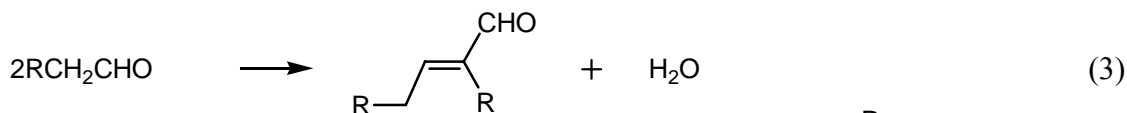
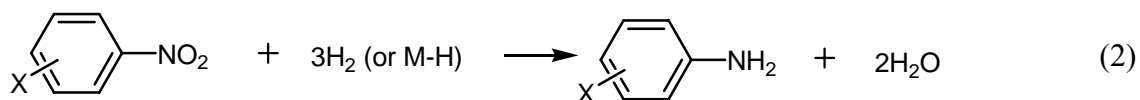


**Figure S4** Direct synthesis of 2-ethyl-3-methylquinoline from nitrobenzene and propanol

Reaction conditions: Nitrobenzene (5 mmol), propanol (20 mL), Ir/TiO<sub>2</sub>-NCs (Ir: 0.167 mol %) at 120 °C under N<sub>2</sub> atmosphere (5 atm).

## 5. Plausible steps involved in the quinoline formation.



**Scheme S1** Plausible steps involved in the quinoline formation

## 6. Characterization of the quinolines

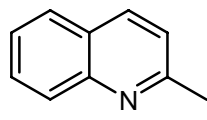


(Table 1, entry 1).<sup>[S5]</sup> <sup>1</sup>H-NMR (CDCl<sub>3</sub>, 500 MHz) δ 8.02 (d, *J* = 8.5 Hz, 1H), 7.97 (d, *J* = 8.5 Hz, 1H), 7.72 (d, *J* = 8.0 Hz, 1H), 7.67 (td, *J* = 7.5, 1.0 Hz, 1H), 7.44 (t, *J* = 7.5 Hz, 1H), 7.22 (d, *J* = 8.5 Hz, 1H), 2.72 (s, 3H).

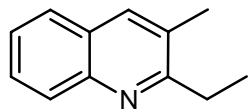


(Table 1, entry 2, 15).<sup>[S5]</sup> <sup>1</sup>H-NMR (CDCl<sub>3</sub>, 500 MHz) δ 8.02 (d, *J* = 8.5 Hz, 1H), 7.82 (s, 1H), 7.69 (d, *J* = 8 Hz, 1H), 7.60 (t, *J* = 7.5 Hz, 1H), 7.43 (t, *J* = 7.5 Hz, 1H), 2.99 (q, *J* = 7.5 Hz, 2H), 2.47 (s, 3H), 1.37 (t, *J* = 7.5 Hz, 3H).

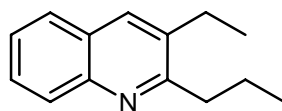


(Table 1, entry 3).<sup>[S5]</sup> <sup>1</sup>H-NMR (CDCl<sub>3</sub>, 500 MHz) δ 8.02 (d, *J* = 8.5 Hz, 1H), 7.85 (s, 1H), 7.71 (d, *J* = 8.0 Hz, 1H), 7.60 (t, *J* = 7.0 Hz, 1H), 7.43 (t, *J* = 7.5 Hz, 1H), 2.97-2.94 (m, 2H), 2.83 (q, *J* = 7.5 Hz, 2H), 1.87-1.80 (m, 2H), 1.33 (t, *J* = 7.5 Hz, 3H), 1.07 (t, *J* = 7.5 Hz, 3H).

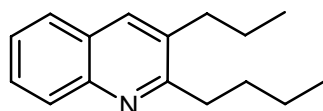


(Table 1, entry 4).<sup>[S5]</sup> <sup>1</sup>H-NMR (CDCl<sub>3</sub>, 500 MHz) δ 8.01 (d, *J* = 8.0 Hz, 1H), 7.84 (s, 1H), 7.71 (d, *J* = 8.0 Hz, 1H), 7.60 (t, *J* = 7.5 Hz, 1H), 7.44 (t, *J* = 7.5 Hz, 1H), 2.98 (t, *J* = 8.0 Hz, 2H), 2.77 (t, *J* = 8.0 Hz, 2H), 1.80-1.72 (m, 4H), 1.53-1.48 (m, 2H), 1.05 (t, *J* = 7.5 Hz, 3H), 0.98 (t, *J* = 7.5 Hz, 3H).

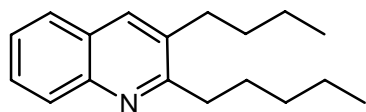


(Table 1, entry 5).<sup>[S6]</sup> <sup>1</sup>H-NMR (CDCl<sub>3</sub>, 500 MHz) δ 8.01 (d, *J* = 8.5 Hz, 1H), 7.84 (s, 1H), 7.71 (d, *J* = 8.0 Hz, 1H), 7.60 (t, *J* = 7.5 Hz, 1H), 7.44 (t, *J* = 7.5 Hz, 1H), 2.97 (t, *J* = 8.0 Hz, 2H), 2.79 (t, *J* = 8.0 Hz, 2H), 1.83-1.77 (m, 2H), 1.71-1.65 (m, 2H), 1.49-1.37 (m, 6H), 0.99 (t, *J* = 7.5 Hz, 3H), 0.92 (t, *J* = 7.5 Hz, 3H).

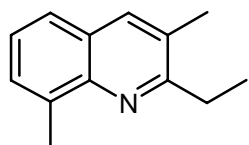


(Table 1, entry 6).<sup>[S5]</sup> <sup>1</sup>H-NMR (CDCl<sub>3</sub>, 500 MHz) δ 7.75 (s, 1H), 7.52 (d, *J* = 8.0 Hz, 1H), 7.44 (d, *J* = 6.5 Hz, 1H), 7.31 (t, *J* = 7.5 Hz, 1H), 2.97 (q, *J* = 7.5 Hz, 2H), 2.80 (s, 3H), 2.44 (s, 3H), 1.42 (t, *J* = 7.5 Hz, 3H).

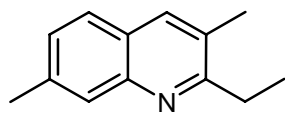


(Table 1, entry 7).<sup>[SS]</sup> <sup>1</sup>H-NMR (CDCl<sub>3</sub>, 500 MHz) δ 7.81 (s, 1H), 7.75 (s, 1H), 7.57 (d, *J* = 8.5 Hz, 1H), 7.26 (d, *J* = 7.5 Hz, 1H), 2.96 (q, *J* = 7.5 Hz, 2H), 2.52 (s, 3H), 2.44 (s, 3H), 1.36 (t, *J* = 7.5 Hz, 3H).

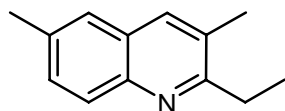


(Table 1, entry 8).<sup>[SS]</sup> <sup>1</sup>H-NMR (CDCl<sub>3</sub>, 500 MHz) δ 7.91 (d, *J* = 8.5 Hz, 1H), 7.75 (s, 1H), 7.45-7.43 (m, 2H), 2.98 (q, *J* = 7.5 Hz, 2H), 2.50 (s, 3H), 2.47 (s, 3H), 1.36 (t, *J* = 7.5 Hz, 3H).

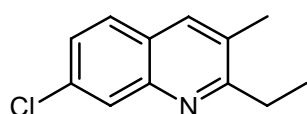


(Table 1, entry 9).<sup>[SS]</sup> <sup>1</sup>H-NMR (CDCl<sub>3</sub>, 500 MHz) δ 8.02 (s, 1H), 7.79 (s, 1H), 7.62 (d, *J* = 8.5 Hz, 1H), 7.39 (dd, *J* = 9.0, 2.0 Hz, 1H), 2.97 (q, *J* = 7.5 Hz, 2H), 2.46 (s, 3H), 1.37 (t, *J* = 7.5 Hz, 3H).

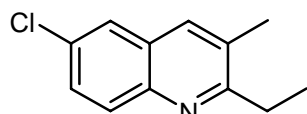


(Table 1, entry 10).<sup>[SS]</sup> <sup>1</sup>H-NMR (CDCl<sub>3</sub>, 500 MHz) δ 7.94 (d, *J* = 8.5 Hz, 1H), 7.74 (s, 1H), 7.67 (d, *J* = 2.0 Hz, 1H), 7.54 (dd, *J* = 9.0, 2.0 Hz, 1H), 2.97 (q, *J* = 7.5 Hz, 2H), 2.48 (s, 3H), 1.37 (t, *J* = 7.5 Hz, 3H).

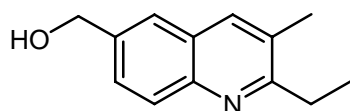


(Table 1, entry 11). <sup>1</sup>H-NMR (CDCl<sub>3</sub>, 500 MHz) δ 7.99 (d, *J* = 8.5 Hz, 1H), 7.81 (s, 1H), 7.65 (s, 1H), 7.59 (d, *J* = 8.5 Hz, 1H), 4.66 (s, 2H), 2.99 (q, *J* = 7.5 Hz, 2H), 2.48 (s, 3H), 1.37 (t, *J* = 7.5 Hz, 3H). <sup>13</sup>C-NMR (CDCl<sub>3</sub>, 125 MHz) δ 163.1, 146.3, 136.1, 135.7, 129.5, 128.6, 128.1, 127.1, 124.9, 72.6, 29.5, 19.1, 12.8 ppm.

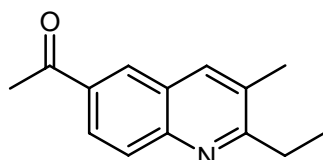


(Table 1, entry 12).<sup>[S7]</sup> <sup>1</sup>H-NMR (CDCl<sub>3</sub>, 500 MHz) δ 8.34 (d, *J* = 1.5 Hz, 1H), 8.16 (dd, *J* = 8.5, 1.5 Hz, 1H), 8.05 (d, *J* = 9.0 Hz, 1H), 7.93 (s, 1H), 3.01 (q, *J* = 7.5 Hz, 2H), 2.71 (s, 3H), 2.51 (s, 3H), 1.39 (t, *J* = 7.5 Hz, 3H). <sup>13</sup>C-NMR (CDCl<sub>3</sub>, 125 MHz) δ 197.6, 166.0, 148.6, 136.9, 134.1, 130.6, 129.0, 128.8, 126.6, 126.4, 29.6, 26.7, 19.1, 12.5 ppm.

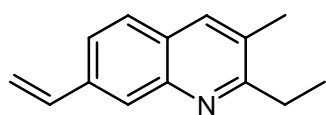


(Table 1, entry 13).  $^1\text{H-NMR}$  ( $\text{CDCl}_3$ , 500 MHz)  $\delta$  7.97 (s, 1H), 7.73 (s, 1H), 7.61 (d,  $J = 8.5$  Hz, 1H), 7.55 (dd,  $J = 8.5, 1.5$  Hz, 1H), 6.88 (dd,  $J = 17.5, 11.0$  Hz, 1H), 5.90 (d,  $J = 17.5$  Hz, 1H), 5.34 (d,  $J = 11.0$  Hz, 1H), 2.96 (q,  $J = 7.5$  Hz, 2H), 2.43 (s, 3H), 1.36 (t,  $J = 7.5$  Hz, 3H).  $^{13}\text{C-NMR}$  ( $\text{CDCl}_3$ , 125 MHz)  $\delta$  163.5, 146.8, 137.5, 136.7, 135.3, 129.2, 126.9, 126.7, 126.5, 123.2, 114.7, 29.4, 19.0, 12.7 ppm.

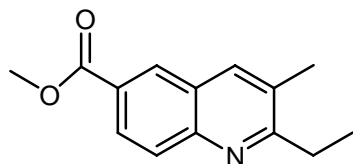
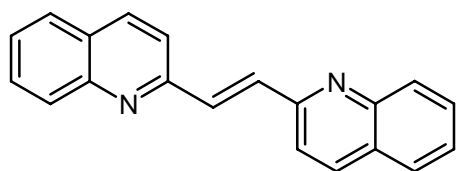


(Table 1, entry 14).  $^1\text{H-NMR}$  ( $\text{CDCl}_3$ , 500 MHz)  $\delta$  8.47 (d,  $J = 1.5$  Hz, 1H), 8.20 (dd,  $J = 9.0, 2.0$  Hz, 1H), 8.04 (d,  $J = 9.0$  Hz, 1H), 7.91 (s, 1H), 3.98 (s, 3H), 3.01 (q,  $J = 7.5$  Hz, 2H), 2.50 (s, 3H), 1.39 (t,  $J = 7.5$  Hz, 3H).  $^{13}\text{C-NMR}$  ( $\text{CDCl}_3$ , 125 MHz)  $\delta$  166.9, 165.8, 148.6, 136.7, 130.4, 129.9, 128.8, 127.9, 127.1, 126.4, 52.2, 29.7, 29.6, 19.1, 12.5 ppm.



(Scheme 1)<sup>[88]</sup>  $^1\text{H-NMR}$  ( $\text{CDCl}_3$ , 500 MHz)  $\delta$  8.13 (dd,  $J = 16.5, 8.5$  Hz, 4H), 7.93 (s, 2H), 7.80-7.78 (m, 4H), 7.73-7.69 (m, 2H), 7.53-7.49 (m, 2H).  $^{13}\text{C-NMR}$  ( $\text{CDCl}_3$ , 125 MHz)  $\delta$  155.3, 148.3, 136.5, 134.6, 129.8, 129.4, 127.6, 127.5, 126.5, 119.5 ppm.

## 7. References

- [S1] M. Haruta, *Catal. Today* **1997**, *36*, 153-166.
- [S2] C. Perez-Melero, A. B. S. Maya, B. D. Rey, R. Pelaez, E. Caballero, M. Medarde, *Bioorg. Med. Chem.* **2004**, *14*, 3771-3774.
- [S3] B. Ravel, M. Newville, *J. Synchrotron Rad.* **2005**, *12*, 537-541.
- [S4] O. Alexeev, B. C. Gates, *J. Catal.* **1998**, *176*, 310-320.
- [S5] Y. Watanabe, S. C. Shim, T. Mitsudo, *Bull. Chem. Soc. Jpn.* **1981**, *54*, 3460-3465.
- [S6] C. S. Cho, W. X. Ren, N. S. Yoon, *J. Mol. Catal. A* **2009**, *299*, 117-120.
- [S7] C. S. Cho, J. S. Kim, B. H. Oh, T.-J. Kim, S. C. Shim, N. S. Yoon, *Tetrahedron* **2000**, *56*, 7747-7750.
- [S8] M. A. Fakhfakh, A. Fournet, E. Prina, J. F. Mouscadet, X. Franck, R. Hocquemiller, B. Figadere, *Bioorg. Med. Chem.* **2003**, *11*, 5013-5023.

*Appendix I*

Spectral copies of  $^1\text{H}$  and  $^{13}\text{C}$  NMR of obtained compounds in this study

